Structure of the unbound nucleus ^{13}Be: One-neutron knockout reaction data from ^{14}Be analyzed in a holistic approach

Yu. Aksyutina,[1] T. Aumann,[1,2] K. Boretzky,[1] M. J. G. Borge,[3] C. Caesar,[1,2] A. Chatillon,[1] L. V. Chulkov,[1,4]
D. Cortina-Gil,[5] U. Datta Pramanik,[6] H. Emling,[1] H. O. U. Fynbo,[7] H. Geissel,[1] G. Ickert,[1] H. T. Johansson,[8] B. Jonson,[8]
R. Kulessa,[9] C. Langer,[1] T. LeBleis,[1] K. Mahata,[1] G. Münzenberg,[1] T. Nilsson,[8] G. Nyman,[8] R. Palit,[10] S. Paschalis,[2]
W. Prokopowicz,[1] R. Reifarth,[1,10] D. Rossi,[1] A. Richter,[2] K. Riisager,[7] G. Schrieder,[2] H. Simon,[1] K. Sümmerer,[1]
O. Tengblad,[3] H. Weick,[1] and M. V. Zhukov[8]

[1]*GSI Helmholtzzentrum für Schwerionenforschung GmbH, ExtreMe Matter Institute, EMMI, D-64291 Darmstadt, Germany*
[2]*Institut für Kernphysik, Technische Universität, D-64289 Darmstadt, Germany*
[3]*Instituto de Estructura de la Materia, CSIC, E-28006 Madrid, Spain*
[4]*Kurchatov Institute, RU-123182 Moscow, Russia*
[5]*Universidade de Santiago de Compostela, 15782 Santiago de Compostela, Spain*
[6]*Saha Institute of Nuclear Physics, 1/AF Bidhannagar, Kolkata IN-700064, India*
[7]*Department of Physics and Astronomy, University of Aarhus, DK-8000 Aarhus, Denmark*
[8]*Fundamental Fysik, Chalmers Tekniska Högskola, SE-41296 Göteborg, Sweden*
[9]*Instytut Fisiki, Uniwersytet Jagielloński, PL-30-059 Kraków, Poland*
[10]*Institut für Kernphysik, Johann-Goethe-Universität, D-60486 Frankfurt, Germany*

At the ALADIN-LAND setup at GSI the unbound nucleus ^{13}Be has been produced in one-neutron knockout reactions from a 304 MeV/nucleon relativistic beam of ^{14}Be ions impinging on a liquid hydrogen target. An analysis of the data including all available information about ^{13}Be, and in particular recent data from a similar experiment performed at RIKEN, has been performed. A consistent description is reached. It is found that the excitation spectrum is dominated by s-waves at low energy, which solves problems from previous seemingly contradictory interpretations. A possible interference between two s-states in ^{13}Be is also discussed. The results indicate that the ground-state wave function of ^{14}Be is dominated by valence neutrons in the s-shell contributing with 60–75% of the total neutron knockout cross section.

I. INTRODUCTION

During the past three decades nuclear physics research has become more and more directed towards the understanding of the intricate properties of nuclei in the drip-line regions. A key ingredient in this endeavor is the continuous, painstaking, and often ingenuous development of techniques to identify, isolate, and manipulate exotic nuclear species. The availability of vast amounts of exotic nuclei, studied both *in situ* and as energetic radioactive beams, has provided a multitude of experimental information building the base for a deeper understanding of their properties. Novel detector techniques and new, powerful analysis methods have been key ingredients. At the same time theory has experienced an unprecedented development hand in hand with the experimental progress. The state-of-the art of the technical progress, the experimental information and the most recent theoretical developments in this field of nuclear physics was recently highlighted in a Nobel Symposium entitled "Physics with Radioactive Beams" [1].

Over three decades, there has been a particular focus on the lightest elements. In fact, all bound isotopes up to the element oxygen have been identified and subject to a multitude of different experimental and theoretical investigations. There has also been a strong interest in unbound nuclei (for recent reviews see Refs. [2,3]), which in some cases are situated in-between bound nuclei, like ^{10}Li or even beyond the last bound isotope like, ^{12,13}Li [4] or ^{16}Be [5]. It is an experimental

challenge to unravel the quantum properties of these unbound systems, which are not trivially distinguished from any debris from the original beam or the subsequent production process. The unbound nuclei also have a central role in the theoretical studies of open quantum systems [6].

The present paper deals with a new one-neutron knockout experiment from ^{14}Be, which is a very rare isotope that has been identified as a two-neutron halo nucleus [7] with a Borromean structure [8]. The produced unbound subsystem, ^{13}Be, has over the years been studied in many different experiments. It is fair to state that none of these experiments alone my be considered as decisive. We have therefore adopted a holistic approach where all existing data are scrutinized and used in our analysis. In this way we have arrived at a consistent interpretation of the nuclear structure of the unbound nucleus ^{13}Be, with all existing data included.

The paper is organized as follows. First a review of the main data concerning ^{13}Be and ^{14}Be is presented. Then the present experiment is described followed by an outline of the analysis of the one-neutron knockout data in a hydrogen target. In this analysis data from other experiments on ^{13}Be are included. In particular, we perform a parallel analysis of the new data presented here together with recent data from RIKEN [9,10]. It is shown that this allows a firm conclusion of the level order in ^{13}Be and demonstrates that all data may be put under a common interpretation without any controversy.

II. SCIENTIFIC BACKGROUND

The element beryllium is, with its six particle-stable isotopes, very rich in scientific challenges. The lightest isotope, ^{7}Be, is well known for its role in the solar neutrino problem. Between ^{7}Be and the stable ^{9}Be, one finds ^{8}Be, consisting of a pair of α particles unbound with 92 keV only. Its role in the triple α reaction for the ^{12}C nuclear synthesis, which has attracted renewed interest in recent years (see Ref. [11] and references therein), is well known.

The ground state of ^{9}Be can be regarded as composed of a $p_{3/2}$-wave neutron plus an ^{8}Be core with 46% in the 0^+ ground state and 54% in the 2^+ state [12]. The first excited state with spin-parity $I^\pi = 1/2^+$ in ^{9}Be [13] can be considered to be a genuine three-body $\alpha + \alpha + n$ resonance, in spite of its decay with emission of an s-wave neutron and with the vanishing potential barrier (see Ref. [14] and references therein).

For ^{10}Be strong $(2^+ \to 0^+)$ $E2$ transitions suggest collectivity [15], which contributes essentially to the famous parity inversion between the ground state and the lowest excited state at 320 keV in ^{11}Be [16,17]. This nucleus in a one-neutron halo nucleus, ^{11}Be, where the ground-state wave function has an $\sim 80\%$ $[^{10}\text{Be}(0^+) \otimes (1s_{1/2})]_{1/2^+}$ component together with some 10–20% $[^{10}\text{Be}(2^+) \otimes (0d_{5/2})]_{1/2^+}$ [18,19].

The ground-state structure of ^{12}Be exhibits almost equal weights of $(1s_{1/2})^2$, $(0p_{1/2})^2$, and $(0d_{5/2})^2$ components (Ref. [20] and references therein). This was recently confirmed experimentally from the observed anomaly in the mass dependence of nuclear charge radii [21].

It is important to note, that adding an extra neutron to the ^{11}Be system depolarizes its core, which enhances the probability that ^{10}Be remains in its ground state [22]. Thus an inert-core three-body model gives a reasonable description of the ^{12}Be structure, concerning its ground and excited bound states, its electromagnetic dissociation and the ^{10}Be-n relative-energy spectrum after fragmentation on a light target [22,23].

However, the existing experimental data for the heaviest particle-stable Be isotope, ^{14}Be $(T_{1/2} = 4.35 \text{ ms})$, namely its binding energy, radius and electromagnetic dissociation spectrum cannot be reproduced within a three-body model consisting of an inert ^{12}Be core interacting with valence nucleons via an ℓ-dependent potential [24]. Within such models, the binary subsystem ^{13}Be either has to be bound or its $0d_{5/2}$ resonance has to have a lower energy than observed experimentally [25,26]. In order to reproduce the two-neutron separation energy in ^{14}Be, Labiche *et al.* [27] assumed an inversion of $0p_{1/2}$ and $1s_{1/2}$ shells in ^{13}Be and tuned the position of $0d_{5/2}$ resonances in accordance with the experimental values. Another approach for ^{14}Be was to employ a three-body model with a ^{12}Be core excitation. The excited core component was approximately 35% [28] which is in contrast with the results given in Ref. [22].

Thus, a simultaneous description of the Borromean nucleus ^{14}Be and its unbound subsystem ^{13}Be still remains a challenge.

TABLE I. Resonance parameters for ^{13}Be obtained in experiments performed with the missing-mass method.

Reaction Reference	E_r / Γ MeV $1/2?$	E_r / Γ MeV $5/2^+$	E_r / Γ MeV $1/2^-$	E_r / Γ MeV $3/2^-; 5/2^+$
^{14}C(^{7}Li,^{8}B),		1.8(5)		
82 MeV, [29]		0.9(5)		
^{14}C(π^-, p),	0.65(10)	1.87(10)	2.95(10)	4.96(20)
stopped π^-,	0.25	0.3(1)	<0.15	1.7
[30]				
^{14}C(^{11}B,^{12}N),	0.80(9)	2.02(9)	2.90(9)	4.94(9); 5.89(14)
190 MeV, [31]	0.4	0.4	0.4	0.4
^{13}C(^{14}C,^{14}O),		2.01(5)		5.13(7)
337 MeV, [32]		0.3(2)		0.4(2)
^{2}H(^{12}Be,p),		2		5
72A MeV, [33]				

III. DISAGREEMENT BETWEEN THE INTERPRETATIONS OF DIFFERENT ^{13}BE EXPERIMENTAL DATA

The first experiment [29] identifying the unbound nucleus ^{13}Be was performed in 1983. In a multi-nucleon transfer reaction, ^{14}C(^{7}Li,^{8}B) a narrow resonance was identified using the missing-mass method. This first result was later confirmed in a variety of experiments employing different reactions [30–33], experiments where also other resonances in ^{13}Be were identified. A summary of these early results is given in Table I.

A consistent result in all these experiments is that there is one resonance at about 2 MeV, as shown in Table I. The weighted mean value from the first four experiments in Table I gives $\bar{E}_r = 1.99(4)$ MeV and the scatter of the experimental E_r values is small ($\chi^2/N = 0.62$, see Fig. 1). The general consensus is that this resonance is an excited state in ^{13}Be with spin-parity $I^\pi = 5/2^+$.

The momentum matching conditions for multinucleon transfer reactions give a considerable enhancement of the cross section for excitation of states with high angular-momentum ℓ. The second intense resonance, which might be a second $5/2^+$ state or a group of overlapping resonances, is found around 5 MeV. On the other hand, the momentum mismatch makes the cross sections smaller for excitation of states with lower ℓ. Such states may be the ones observed at 0.8 MeV and at 2.9 MeV [30,31] and might therefore be considered as $\ell \leqslant 1$ states. However, the experimental resolution in these experiments did not allow to determine whether the state at 0.8 MeV has $I^\pi = 1/2^+$ or $I^\pi = 1/2^-$ [31], based on the spectral shape.

With the advent of energetic beams of radioactive nuclei, which can induce nuclear reactions, new and better possibilities for investigation of drip-line nuclei has become available (for a recent review see Ref. [34]). The invariant-mass method, where momenta of the decay particles are measured in coincidence to determine the relative-energy, E_{fn}, between fragment and neutron, is applied in the most recent experiments.
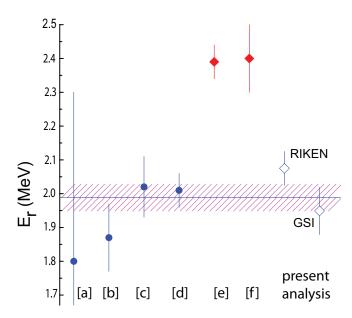
FIG. 1. (Color online) Resonance energy of the state at $\sim$2 MeV in ^{13}B observed in experiments utilizing the missing-mass method (circles) and the invariant-mass method (rhombuses). The energies are from [a] [29], [b] [30], [c] [31], [d] [32] [e] [35], and [f] [9]. The results of the present analysis are shown as open rhombuses. The solid line shows the error weighted average value for the resonance, E_r, of missing-mass experiments only, were the overlaid hatched area shows the uncertainty.
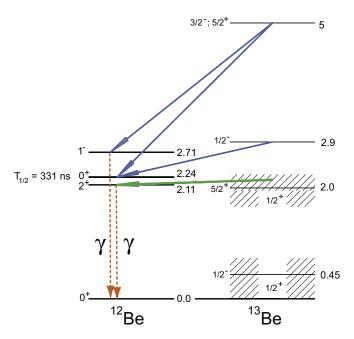

FIG. 2. (Color online) Level scheme of states in ^{13}Be. The arrows show possible decays to excited states in ^{12}Be and the horizontal lines indicate the position of the $\ell > 0$ resonances. Note that the feeding of the 2^+ state in ^{12}Be at 2.11 MeV is energetically allowed only from the upper tail of the $5/2^+$ resonance at 2 MeV in ^{13}Be.

It is surprising that the ^{13}Be excitation-energy spectra obtained, either in proton stripping from ^{14}B [35,36] or in neutron stripping from ^{14}Be, Refs. [9,10,37], look very different from those obtained with the missing mass approach [30–33]. The spectra obtained after neutron-stripping reactions are dominated by an asymmetric, intense broad peak with a relative energy around 0.5 MeV. Apart from a less pronounced maximum around 3 MeV there is no other resonance structures observed in the spectra at higher energy. The nuclear structure of the projectiles and an insufficiency of the invariant-mass method might be the origin of this difference.

The main problem with the invariant mass method, without gamma-ray detection, is that neutron emission to final particle-bound excited states in the daughter nucleus cannot be distinguished from transitions to the ground state. This means that the peak in the relative-energy spectrum, $d\sigma/dE_{fn}$, becomes shifted towards lower energies due to the excitation energy of the state.

The possible ^{13}Be decay branches to excited states in ^{12}Be are shown in Fig. 2. The γ rays from 2^+ and 1^- states in ^{12}Be, detected in coincidence with neutrons, were observed in an experiment performed at RIKEN [9,10]. The $d\sigma/dE_{fn}$ spectrum in coincidence with γ rays shows the presence of a decay branch from a $5/2^+$ state in ^{13}Be to the 2^+ state in ^{12}Be via emission of an s-wave neutron. In addition, coincidences observed between neutrons and 2.7 MeV γ rays from the 1^- state can be explained as originating in decay from the state at $E_r = 5.2(1)$ MeV, $\Gamma = 1.4(2)$ MeV. This might be due to s-wave neutron emission from an $I^\pi = 3/2^-$ state. From the triple coincidences between 2.1 MeV γ rays, ^{12}Be,

and neutrons up to $E_{rel} = 5$ MeV, the integrated cross section amounts to 9.6(5) mb, while the triple coincidences with 2.7 MeV γ rays gives 3.5(10) mb for the 69 MeV/nucleon ^{14}Be beam impinging on a hydrogen target [10].

The isomeric state 0_2^+ in ^{12}Be has a long lifetime [38], which renders the in-beam γ-ray coincidence technique inapplicable. Transitions to this state might therefore only appear as two ghost peaks in the $d\sigma/dE_{fn}$ spectrum at about 0.7 and 2.8 MeV.

One more long-lived 0^- state in ^{12}Be, has been predicted [23] at an excitation energy around 2.7 MeV. A recent experiment [39] at the REX ISOLDE facility at CERN, using an ^{11}Be(d, p) transfer reaction gives, however, no evidence for the existence of such a state.

There are also states with a large component of the ^{12}Be ground state plus one neutron, which might have twins with strong ^{12}Be$(0_2^+) + n$ components. Hence, ^{13}Be could be expected to have a second $5/2^+$ state around 5 MeV and a second $1/2^+$ close to the position of the second 0^+ state in ^{12}Be (see Fig. 2).

A great deal of controversy has until now existed concerning the interpretations of experimental spectra obtained using the invariant-mass method, as illustrated in Table II. A dominant s wave can be expected at low relative energy E_{fn}, since the weight of an s-shell configuration in the structure of both ^{14}Be and ^{14}B, is large [40–42]. However, contradictory interpretations of the low energy spectrum were given in Refs. [9,10,35–37]. From the proton knockout data obtained at GANIL [35,36] it was proposed to be a Breit-Wigner $\ell = 0$ resonance. The interpretation made from the one-neutron knockout data from ^{14}Be, measured at GSI, was that it was dominated

TABLE II. Resonance parameters for ^{13}Be obtained in experiments performed with the invariant-mass method.

Reaction Reference	a_S or E_r/Γ fm or MeV $1/2^+$	E_r/Γ MeV $1/2^-$	E_r/Γ MeV $5/2^+$	E_r/Γ MeV $1/2^-$	E_r/Γ MeV $3/2^-; 5/2^+?$
C(^{14}Be,^{12}Be $+ n$),	$-3.2^{0.9}_{1.1}$	0.41(8)	2.0[a]	3.0[a]	5.0[a]
287 MeV/nucleon, [37]		0.4(5)	0.3	0.4	1.5
C(^{14}B,^{12}Be $+ n$),	0.70(5)		2.4(1)		
35 MeV/nucleon, [35,36]	1.7(1)		0.6(2)		
^{1}H(^{14}Be,^{12}Be $+ n$),	$-3.4(6)$	0.51(1)	2.39(5)		
68 MeV/nucleon [9]		0.45(3)	2.4(2)		

[a]Resonance parameters were taken from multinucleon transfer experiments and kept fixed.

by a virtual s-state [37], and recently it was interpreted as a $\ell = 1$ resonance from data obtained at RIKEN [9,10].

Furthermore, the $5/2^+$ state in Refs. [9,10,35] was found at $E_r = 2.4$ MeV, which is more than 3σ higher than that derived from missing-mass experiments (see Fig. 1). While the width of this state obtained at GANIL [35] is in agreement with the earlier experiments, $\Gamma = 0.6(2)$ MeV, the RIKEN data [10] gave a four times larger value, $\Gamma = 2.4(2)$ MeV (see Table II). For the channel radius $R_{ch} = 4.9$ fm used in Ref. [10], the single-particle width becomes $\Gamma_{sp} = 1.0$ MeV (see Eq. 3F-51 in Ref. [43]). Thus the observed width of the state, which was seen in missing-mass experiment as a narrow state, is 2.4 times broader than Γ_{sp} in Ref. [10]. This result is a startling discovery. In the past, various reactions have been used to study the reaction dependence of a resonance decay width. The conclusion was that the resonance widths are self-consistent and indicate little if any reaction dependence, see e.g. Ref. [44] and references therein.

In this paper data from our new experiment, carried out using the same reaction as in [9,10] but at much higher energy, are presented. By combining these data with results obtained in earlier experiments we attempt to find a solution to this apparent controversy.

IV. EXPERIMENTAL SETUP AND RESULTS

The experiment was performed at GSI, Darmstadt, where a ^{14}Be beam was produced in fragmentation reactions of a 360 MeV/nucleon ^{18}O beam from the heavy-ion synchrotron, SIS, in a beryllium production target. The secondary ^{14}Be beam, with an energy of 304 MeV/nucleon, was selected by magnetic analysis in the fragment separator, FRS, and directed towards a liquid-hydrogen target, placed in front of the large-gap dipole magnet spectrometer ALADIN and the large area neutron detector, LAND [45]. The intensity of the ^{14}Be beam was 40 particles s^{-1}, and its divergence at the entrance of the experimental setup was 1.8 mrad in horizontal and 1.5 mrad in vertical direction, respectively.

The liquid hydrogen was kept in a target container (28 mm in diameter and 50 mm long) equipped with thin mylar windows. The target, with an effective thickness of 350 mg/cm^2, was placed in a vacuum chamber. Background measurements were performed with an empty target. The background contribution amounts to 18% for energies below

4 MeV and increases then smoothly with energy to reach 35% at 6 MeV

The polar and azimuthal angles of the charged reaction products were obtained from measurements with two MWPC's. One was placed 900 mm upstream of the target and the second 657 mm downstream. The achieved angular resolution for fragments of about 3.8 mrad had its main origin in uncertainties in the reaction-point determination and in angular straggling in the target material. The angular resolution for neutrons was determined to be 4.2 mrad.

The nuclear charge of the reaction fragments was obtained from the energy losses, ΔE, in pin-diodes, placed directly behind the target and in scintillators in a time-of-flight wall (TOFW) placed at a distance of 529 cm behind the center of the ALADIN magnet. The masses of the fragments were determined by analyzing their magnetic rigidity in ALADIN. The bending angles of the fragments were obtained from the coordinates of the hit in the TOFW.

The neutrons, recorded in coincidence with fragments, were detected in the large area neutron detector LAND, placed 10 m downstream of the target. A dedicated tracking routine was applied to reconstruct the spatial coordinates and thus the momentum of the detected neutron. The routine can resolve several neutrons crossing the LAND detector simultaneously. The characteristics of the developing shower (e.g., the released energy, the opening angle and the extension) exhibit statistical fluctuations, which result in uncertainties in the reconstructed parameters for the detected neutron. The tracking analysis of the experimental data is therefore used together with Monte Carlo simulations, allowing additional corrections of the final result. Detailed information about the neutron-induced charged-particle showers in LAND has been obtained from a calibration measurement [45] using monoenergetic neutrons, produced in deuteron break-up reactions, with energy close to the neutron energies in the present experiment. The response of the LAND detector to a single neutron crossing the detector area is used in the Monte Carlo simulations.

The relative energy in the ^{12}Be $+ n$ system, often referred to as the invariant mass, was calculated using the relativistic equation:

$$E_{fn} = \|\mathbf{P}_f + \mathbf{P}_n)\| - M_f - m_n, \tag{1}$$

where $\mathbf{P}_f$ ($\mathbf{P}_n$) and M_f (m_n) are momentum four vectors and masses of the fragment (neutron), respectively.

The experimental resolution of the relative-energy spectra was obtained from Monte-Carlo simulations using the measured detector responses. The resolution (FWHM) is about 250 keV at 500 keV and increases to about 700 keV at 2 MeV. The Monte Carlo simulations also give the detection efficiency. The efficiency remains nearly constant, 85%, up to $E_{fn} = 2$ MeV and decreases at higher energies due to the finite solid angle of the neutron detector and the ALADIN acceptance. All measured distributions have been corrected for efficiency. The experimental data were also corrected for two-neutron events wrongly identified as one-neutron events.

V. ANALYSIS

A. Relative-energy spectra $d\sigma/dE_{fn}$

In this section the analysis of the relative-energy spectrum, $d\sigma/dE_{fn}$, from this experiment, shown in Fig. 3(b), is presented. The new data have better energy resolution and higher statistics than those obtained in our earlier work from 2007 [37]. At the onset one may here point out that the complexity of the analysis of unbound nuclear systems increase drastically with charge and mass. It is therefore not advisable to look at each individual case separately. We have consequently adopted an approach where we use essentially all earlier information, not only as inputs but we also expose them to a similar, joint analysis. For this reason it is very important for our later conclusions that we have been able to
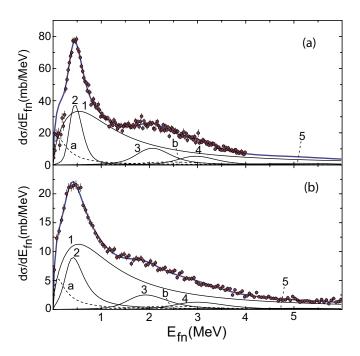

FIG. 3. (Color online) (a) ^{12}Be $+ n$ relative-energy spectrum from the neutron-knockout reaction ^{1}H(^{14}Be,^{12}Be $+ n$) at 69 MeV/nucleon from Ref. [9]. The fit made in the region $E_r \geqslant 0.25$ MeV gave $\chi^2/N = 1.2$. (b) Relative-energy from the present experiment at an energy of 304 MeV/nucleon. The fit gave $\chi^2/N = 0.91$. The different curves display the decomposition of the spectrum into individual resonances. The individual components in the fit are marked according to the description in the text.

get access to original data from our colleges at RIKEN, while the data from the GANIL experiment could be extracted from Ref. [36]. We are therefore able to proceed with the analysis process by working with our own data in parallel with those from Refs. [9,29–32,35–37].

One important issue here is that we, in the course of our work, have found that our earlier description of the low-energy peak, as a virtual s state according to the prescription in Ref. [17], may meet problems in the analysis of the new data. Moreover, there are indications from the proton-knockout data from ^{14}B that the main peak in these data is an s-wave resonance state [36].

For these reasons we have adopted Breit-Wigner resonance shapes for all partial waves that are included in the analysis according to the following expression:

$$\frac{d\sigma}{dE_{fn}} \sim \frac{\Gamma(E_{fn})}{(E_{fn} - E_r)^2 + \frac{1}{4}\Gamma^2(E_{fn})}. \tag{2}$$

The dependence of the resonance width $\Gamma(E_{fn})$ on the relative energy and on the angular momentum were taken into account as in Ref. [46].

The low-energy peak observed in the relative-energy spectra shown in Refs. [9,37] as well as in the present experiment is more narrow than the one observed from the data presented in Ref. [36], where states of ^{13}Be were populated after proton knockout from ^{14}B. One may imagine two alternative explanations for this difference:

(i) The relative-energy distribution might be smeared out due to the large momentum transfer to the core nucleus in the knockout of a tightly bound proton, $S_p(^{14}$B$) = 16.87(7)$ MeV [47]. Such an effect has been observed earlier for the ^{8}He $+ n$ system produced in proton knockout from ^{11}Li [48].

(ii) A narrow $1/2^-$ state may exist in ^{13}Be at low energy [49]. The structure of ^{14}B has the main configuration ^{13}B$(3/2^-) \otimes (sd)$ [40], which means that only s and d states in ^{13}Be should be populated significantly in proton knockout while the $1/2^-$ state can appear after neutron knockout from ^{14}Be.

In this analysis we temporarily stick to the latter explanation, which means that we assume that there is no population of a low-lying $1/2^-$ state in the GANIL experiment [36].

We now proceed with the analysis starting with the $d\sigma/dE_{fn}$ spectrum, obtained in proton knockout [36] where one expects a rather clean $1/2^+$ shape at low energy. A fit was made with the following assumptions:

(i) a Breit-Wigner $\ell = 0$ resonance and
(ii) two narrow resonances at the energies 2.1 MeV ($\ell = 2$) and 2.9 MeV ($\ell = 1$), respectively.

The acceptance and experimental resolution were taken from Ref. [36]. A satisfactory description of the spectrum was obtained with $E_r = 0.81(6)$ MeV and $\Gamma = 2.1(3)$ MeV. The parameters for the other resonances were close to those known from the missing-mass experiments (see Table I). From this analysis one finds that the $5/2^+$ state contributes with 16% and the 2.9 MeV state with 7%. From now on we use the obtained

values for E_r and Γ for the $1/2^+$ state (in the following referred to as component 1) as fixed input parameters in the analysis.

The next set of input data used in the fitting of our relative-energy spectrum was obtained from the $d\sigma/dE_{fn}$ spectrum for ^{12}Be + n observed in coincidence with gamma rays from the 2^+ state at 2.1 MeV and and 1^- 2.7 MeV in ^{12}Be [9,10]. These spectra were also fitted using Breit-Wigner shapes. The first spectrum corresponds to neutron emission from the tail of the ^{13}Be($5/2^+$) resonance to the 2^+ state in ^{12}Be [50] (see Fig. 2). The second spectrum corresponds to the decay from a ^{13}Be state at $E_r = 5.2(1)$ MeV [$\Gamma = 1.4(2)$ MeV] to the 1^- state in ^{12}Be (Fig. 2). The shapes of these two spectra were kept fixed and used during the fitting procedure and they are referred to as components a and b, respectively. In the analysis of the spectrum obtained at RIKEN, the cross sections for these components were taken to be 9.6 mb and 3.5 mb, respectively [10]. In the analysis of the present experiment, the cross section for component a was treated as a free parameter and component b was scaled down with a factor of 3, which corresponds to the expected ratio of the cross sections at the two energies.

The remaining components used in the fit were based on the following assumptions:

(i) Component 2: A narrow $\ell = 1$ resonance at low E_{fn}, observed earlier in Refs. [9,37], was included with resonance position E_r, resonance width Γ and the cross section σ, as free parameters in the fit.

(ii) Component 3: A narrow $\ell = 2$ resonance identified in missing-mass experiments as a $5/2^+$ state [30–33]. For this resonance E_r and σ were taken as free parameters.

(iii) Component 4: A resonance at around 3 MeV observed in Refs. [30,31] as a $1/2^-$ state. Also here E_r and σ were taken as free parameters.

(iv) Component 5: A resonance structure at around 5 MeV seen in Refs. [30–33]. The fixed parameters are $E_r = 5$ MeV and $\Gamma = 1.5$ MeV and only the cross section was used as a free parameter.

With these input parameters the spectra from RIKEN and the present GSI experiment were fitted simultaneously. The
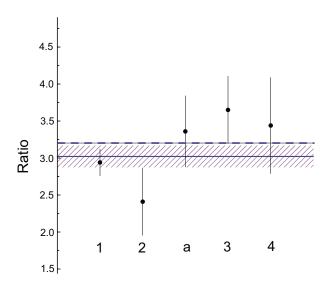

FIG. 4. (Color online) Ratio between experimental cross sections for excitation of ^{13}Be resonances obtained in ^{1}H(^{14}Be,^{12}Be + n) at 69 MeV/nucleon and 304 MeV/nucleon. The obtained ratio 3.0(1) is close to the one given in Ref. [51] shown as the dashed line. The labeling of the resonances is the same as in Fig. 3.

spectrum from RIKEN [9] was analyzed in the energy interval $0.25 \leqslant E_{fn} \leqslant 4$ MeV. The low-energy part with $E_{fn} \leqslant 0.25$, was excluded from the fit since the signal to background ratio was 0.1 there. The spectrum from the present experiment was fitted in its entire energy range $0 \leqslant E_r \leqslant 6$ MeV. The results of the fits to the two spectra are shown in Fig. 3. The numerical values for the obtained parameters are given in Table III.

The validity of the assumption that the reaction mechanism is the same in the two experiments is demonstrated in the last column of the table, where the ratio of the cross sections for the different components in the two spectra are given. They are also displayed in Fig. 4. The error-weighted ratio is 3.0(1), which is close to the ratio of the (p, n) total cross sections at these two energies, which is 3.205(34) [51]. This can be be taken as evidence for the suitability of the impulse-approximation formalism used in the present analysis.

TABLE III. Resonance parameters for ^{13}Be obtained in a simultaneous analysis of the experiments performed at GSI and RIKEN. The last column presents the ratio of cross sections for excitation of different modes obtained in the analysis of the two experiments. Statistical uncertainties are given.

	RIKEN			GSI			Cross-section
	σ, mb	E_r, MeV	Γ, MeV	σ, mb	E_r, MeV	Γ, MeV	ratio
1[a]	66(2)	0.81(6)	2.1(3)	22(1)	0.81(6)	2.1(3)	2.9(2)
2	14(1)	0.46(1)	0.11(2)	6(1)	0.44(1)	0.39(5)	2.4(5)
3	11.1(7)	2.07(3)	0.5[b]	3.0(3)	1.95(5)	0.5[b]	3.6(5)
4	6.2(6)	2.98(4)	0.5[b]	1.8(3)	3.02(9)	0.5[b]	3.4(5)
a[c]	9.6(5)	2.0[b]	0.5[b]	2.8(5)	2.0[b]	0.5[b]	3.4(5)
b[c]	3.5(5)	5.2(1)	1.4(2)	1.17[d]	5.2[b]	1.4[b]	3.0

[a]Resonance parameters were obtained from the fit to the ^{12}Be + n spectrum from Ref. [36].
[b]Resonance parameter was fixed.
[c]Shape of the spectrum was taken from [9,10].
[d]Scaled by factor 3 from [9,10].

Moreover, the observation that the cross-section ratios of the different components stay the same within the statistical uncertainties at two different beam energies further validate the decomposition. Note, that the cross section of neutron knockout from ^{8}He in a hydrogen target was measured earlier at 82 MeV/nucleon [52] and at 240 MeV/nucleon [53]. From the ratio of the (p, n) cross sections at these two energies, one would expect that the cross section at lower energy should be 2.4 times larger [51]. It was, however, found that they are nearly the same. Most likely the use of proton tagging in Ref. [52] caused strong kinematical cuts resulting in a lowering of the neutron knockout cross section.

A Breit-Wigner $\ell = 0$ resonance alone cannot describe the low-energy part of the spectrum. An additional resonance at $E_r \approx 0.45$ MeV (component 2) is needed in both the spectra from Ref. [9] and the present experiment. The requirement of such a component was first shown in Ref. [37] where it was simulated with a Breit-Wigner shape with $\ell = 1$, the same as in Ref. [9] and in the present experiment.

The resonance energies of the narrow resonances [at 2.07(3) MeV and 2.98(4) MeV for RIKEN; 1.95(5) MeV and 3.02(9) MeV for present experiment; see Table III] are within statistical uncertainties the same as obtained by the missing-mass method [30,31] (see Table I and Fig. 1)

The next proof of the validity of the decomposition comes from the cross-section ratio between components labeled as 3 and a in Fig. 3. This ratio has to be the same in both experimental spectra. It should be reminded here that the component a corresponds to the decay of the $5/2^+$ resonance in ^{13}Be to the 2^+ state in ^{12}Be, while component 3 represents the decay of the same ^{13}Be resonance to the ^{12}Be ground state.

B. Momentum distributions and momentum profile $P(E_{fn})$

The impulse approximation for valence-neutron knockout from ^{14}Be, described by a Feynman diagram with two vertices (see, e.g., Ref. [54]), justifies the assumption that the momentum of ^{12}Be $+ n$ system is equal to the momentum of the knocked-out neutron inside the projectile. Also the total spin I of ^{12}Be $+ n$ in the final state is the same as j of the knocked-out neutron. Thus the distribution of ^{12}Be $+ n$ momentum, $\mathbf{P}_{f+n} = \mathbf{p}_f + \mathbf{p}_n$, gives additional information about the quantum numbers for the ^{13}Be resonances. Analytical expressions for longitudinal momentum distributions applicable to neutron halos were deduced within the eikonal approximation employing modified Bessel functions for the asymptotic neutron wave function [55,56]. The transverse momentum components carry essentially the same information.

At relativistic energies, the shapes of the longitudinal and transverse momentum distributions are the same, even in the case of a complex target [57]. We thus apply the formulas from Refs. [55,56] in our further analysis of the experimental momentum distributions.

The experimental transverse momentum distributions obtained from this experiment, $P^x_{f+n} = p^x_f + p^x_n$, in three different energy regions are shown in Fig. 5. The distributions were analyzed using analytical expressions given in Refs. [55,56]. The results of the fit assuming three components, s-, p- and
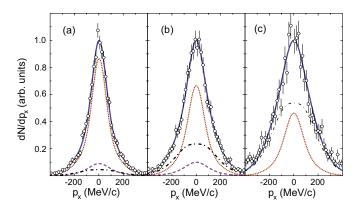

FIG. 5. (Color online) Transverse momentum distributions of the ^{12}Be $+ n$ system from ^{1}H(^{13}Be,^{12}Be $+ n$) at 304 MeV/nucleon obtained in the present experiment. Events were collected in (a) $0.4 \leqslant E_{fn} \leqslant 0.5$ MeV, (b) $1.8 \leqslant E_{fn} \leqslant 2.2$ MeV, (c) $4 \leqslant E_{fn} \leqslant 6$ MeV. Contributions from different ℓ values (s wave as a dotted line, p wave as a dashed line, d wave as a dashed-dotted line) are also shown.

d-waves, are displayed in Fig. 5 and the results are given in Table IV.

A much stronger d-wave component, as compared to the analysis of the $d\sigma/dE_{fn}$ spectrum, is the first difference to be noticed. This result is not surprising, since the applicability of a Breit-Wigner shape for an s-wave resonance is very doubtful, especially at high energies. The fit in the $0.4 \leqslant dE_{fn} \leqslant 0.5$ region indicates that the p-wave component is very small. There are, however, very large statistical uncertainties that prevent a strict conclusion. The reason for the large statistical uncertainties is that the determinations of the parameters become highly correlated. Two variables are nearly collinear, as shown in Fig. 6. The decomposition of the momentum distribution into more than two component is thus an ill-defined problem.

The analysis of the dependence of the momentum-distribution width on the relative energy may give additional information, as first demonstrated in Ref. [50]. This method is based on a study of the variance [or root-mean-square (rms)] of the transverse momentum, P^x_{f+n}, as a function of E_{fn}. Such a distribution is referred to as the momentum-profile function, $P(E_{fn})$.

The experimental momentum-profile function constructed from the ^{12}Be $+ n$ data from this experiment is shown in Fig. 7

TABLE IV. Relative intensities of the s, p, and d components obtained by least-square fits to the measured momentum distributions of the ^{12}Be $+ n$ system in different relative-energy regions, E_{fn}. The distributions were analyzed for transverse momenta from -400 MeV/c to 400 MeV/c.

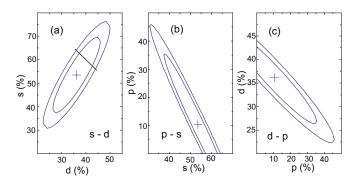| Energy region	s (%)	p (%)	d (%)	χ^2_{min}/N
0.4–0.5 MeV	80(10)	11(15)	8(6)	0.82
1.8–2.2 MeV	53(12)	10(18)	36(7)	0.65
2.6–3.2 MeV	27(15)	36(24)	38(10)	0.92
4.0–6.0 MeV	32(3)	<4	68(3)	1.6

FIG. 6. (Color online) Correlations between the fit components in a least-square fit of the momentum distribution from events in the energy region $1.8 \leqslant E_{fn} \leqslant 2.2$ MeV. (a) s-d, (b) p-s, and (c) d-p. The cross shows the position of $\chi^2_{\min} = 30.4$. The χ^2 stays constant along the contours. $\chi^2 = \chi^2_{\min} + 1$ for inner contours, and $\chi^2 = \chi^2_{\min} + 2$ for outer contours. The contours above the straight solid line correspond to unphysical solutions.

together with the results of model calculations [55,56] for pure s, p, and d waves.

At low energies it is found that the experimental $P(E_{fn})$ distribution is sharply decreasing with increasing energy. This behavior is the result of two overlapping contributions: (i) component 1 with $\ell = 0$ and (ii) component a, originating from the $5/2^+$ state in ^{13}Be populated in knockout of an $\ell = 2$ neutron from ^{14}Be and followed by emission of an $\ell = 0$ neutron to the 2^+ state in ^{12}Be. This decay is energetically only possible from the tail of the $5/2^+$ resonance by emission of low-energy neutrons. Thus the rms momentum corresponds to angular momentum, $\ell = 2$, of the knockout neutron. The 2^+ state in ^{12}Be de-excites by γ emission to the ground state of ^{12}Be. This decay path was identified in the RIKEN experiment [9] from n-γ coincidences.
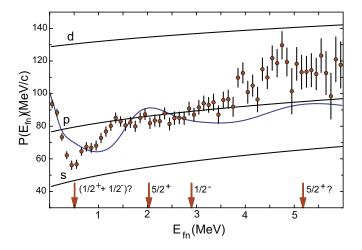

FIG. 7. (Color online) The momentum-profile distribution for the ^{12}Be $+ n$ system after one-neutron knockout from ^{14}Be impinging on a hydrogen target at 304 MeV/nucleon. The arrows indicate the positions of states in ^{13}Be. The theoretical profile functions for s, p, and d waves are shown together with a curve calculated using the relative weights of the different ℓ components obtained from the fit of the relative-energy spectrum (see text).

The momentum profile also shows a minimum close to the dominant peak in $d\sigma/dE_{fn}$. The rms value at the minimum is close to that calculated for an s wave. This observation confirms the validity of the analysis of the relative-energy spectrum, $d\sigma/dE_{fn}$, from the present experiment and those given in Refs. [36,37]. An s-wave dominance in this energy region is therefore settled. This result is also a confirmation of the conclusions from different experiments [41,42,58–60] that there is an s-wave dominance in the ^{14}Be wave function.

The solid curve in Fig. 7 shows the calculated profile function, $P_{\text{calc}}(E_{fn})$, using the relative weights of the different ℓ components obtained from the decomposition of the $d\sigma/dE_{fn}$ spectrum, and has the following analytical form:

$$P^2_{\text{calc}}(E_{fn}) = \rho_s \sigma_s^2 + \rho_p \sigma_p^2 + \rho_d \sigma_d^2, \qquad (3)$$

where σ_ℓ^2, ρ_ℓ are calculated variances and weights obtained from the fit for definite ℓ values, respectively.

The s-wave component in the E_{fn} spectrum is broad and contributes therefore to a large extent in the region around the d state and also towards the energy region above. One finds that an s/d ratio of approximately 70%/30% is needed to explain the rms momentum at $E_{fn} = 2$ MeV.

The decays from higher lying $1/2^-$ and $5/2^+$ states to the long-lived isomeric state in ^{12}Be(0^+_2) were not considered in our analysis. These decays may result in peaks in the E_{fn} spectrum at 0.7 MeV [from the decay of ^{13}Be($1/2^-$) to the 0^+_2 state in ^{12}Be by emission of $\ell = 1$ neutrons] and at $\sim$3 MeV (from the decay of ^{13}Be($5/2^+_2$) at $\sim$5 MeV [32] by emission of $\ell = 2$ neutrons [61]). However, the combined analysis of $d\sigma/dE_{fn}$ and $P(E_{fn})$ shows that the transition from the higher lying $1/2^-$ state cannot be significant.

The disagreement between the theoretical and experimental momentum profile is prominent at around $E_{fn} = 0.5$, where the appearance of an $\ell = 1$ state is expected, and at $E_{fn} \geqslant 4$ MeV, where a contribution from $\ell = 0$ prevails all others, as has been obtained from the $d\sigma/dE_{fn}$ analysis.

The reasons for this could be the existence of a second $1/2^+$ excited state. In the following section we investigate how the existence of two overlapping $\ell = 0$ states in ^{13}Be can influence the result of the analysis.

C. Possible interference between two $\ell = 0$ states in ^{13}Be

The problem with the interpretation of the data has its origin in the complex structure of the neutron-rich beryllium isotopes. It was enunciated already in 1976 that several observed properties of the $T = 2$, $I^\pi = 0^+$ states of $A = 12$ nuclei favor a model in which only small components of the states belong to the lowest shell-model configuration [20]:

$$
\begin{aligned}
^{12}\text{Be}(0^+) = {}& \alpha[^{10}\text{Be} \otimes (1s_{1/2})^2] + \beta[^{10}\text{Be} \otimes (0p_{1/2})^2] \\
& + \gamma[^{10}\text{Be} \otimes (0d_{5/2})^2], \qquad (4)
\end{aligned}
$$

where the ^{10}Be is an inert core with a closed $0p_{3/2}$ shell. This prediction was later confirmed in a series of experiments [15,62–65]. The shell-mixing phenomenon with $\alpha^2 = 0.35$, $\beta^2 = 0.31$, and $\gamma^2 = 0.34$ [20] was interpreted as the breakdown of the $N = 8$ shell closure [62]. A breaking of the

closed-shell structure of the neutrons in ^{12}Be was also suggested in several theoretical papers [20,27,49,66–69].

The weights of the different configurations in the ^{12}Be wave function are almost equal. Thus, the $1/2^+$ state in ^{13}Be cannot be considered as a single-particle state, ^{12}Be$\otimes(1s_{1/2})$. Two few-body $1/2^+$ states are therefore expected in ^{13}Be. The first with the configuration:

$$^{13}\text{Be}(1/2_1^+) = \lambda[^{10}\text{Be} \otimes (0p_{1/2})^2 \otimes (1s_{1/2})]$$
$$+ \mu[^{10}\text{Be} \otimes (0d_{5/2})^2 \otimes (1s_{1/2})]. \quad (5)$$

where ^{10}Be is an inert core with a closed $1p_{3/2}$ shell. The second $1/2^+$ state is orthogonal to the first one:

$$^{13}\text{Be}(1/2_2^+) = \mu[^{10}\text{Be} \otimes (0p_{1/2})^2 \otimes (1s_{1/2})]$$
$$- \lambda[^{10}\text{Be} \otimes (0d_{5/2})^2 \otimes (1s_{1/2})]. \quad (6)$$

In a recent paper Fortune [70] proposed the existence of two $1/2^+$ states in ^{13}Be, the first one at low energy and the second placed 3.12 MeV above the ^{12}Be $+ n$ threshold. The proposed structure of the two resonances are $[^{10}\text{Be}\otimes(0p_{1/2})^2 \otimes (1s_{1/2})]$ and $[^{10}\text{Be}\otimes(0d_{5/2})^2 \otimes (1s_{1/2})]$, respectively. Such a structure is actually similar to Eqs. (5) and (6) with μ close to zero.

The spectroscopic factor (S_d) for the decays of these two states to the ground state of ^{12}Be is given by the overlap integral with the ^{12}Be ground state wave function given in Eq. (4) with the coefficients as given above. For the decay of the first $1/2^+$ state to the ^{12}Be ground state one obtains $S_d = 0.31$, which is in support of the assumption of an $\ell = 0$ resonance shape. For the decay of the second $1/2^+$ state one gets $S_d = 0.34$ to the ^{12}Be ground state and $S_d = 0.02$ for the decay to the 0_2^+ state [20,70]. Thus we would only expect a small contribution from decay to the excited state in ^{12}Be.

This few-body resonance can be considered as an analog to the known second $1/2^+$ state in ^{17}O. A narrow $1/2^+$ state $(\Gamma = 124$ keV) was found experimentally at 2.2 MeV above the neutron-decay threshold.

In the ^{13}Be case, both states are expected to be broad and having strong interference. We shall therefore check if we can replace the description of the low-energy part as a sum of p and s states by the two interfering s states. We follow Ref. [46] and write

$$d\sigma/dE_{fn} \propto \sqrt{E_{fn}} \left| \frac{a_1}{E_1 - E_{fn} - i\Gamma_1/2} \right.$$
$$\left. + \frac{a_2}{E_2 - E_{fn} - i\Gamma_2/2} \right|^2, \quad (7)$$

here E_i (Γ_i) are the resonance energy and energy-dependent resonance width, respectively.

We now proceed with the analysis in the following way. We start by summing the relative energy spectra from the s and p states using the parameters from Table III. This spectrum, shown in Fig. 8(a), is used as our starting point and a fit to it is done using Eq. (7) and an additional Breit-Wigner term to take into account the decay of the second $1/2^+$ state to the 0_2^+ state in ^{12}Be. Further we limit the energy region of the fit to $0 \leqslant E_{fn} \leqslant 3$ MeV. A perfect fit to the spectrum is found with the parameters given in Table V, and with $a_1/a_2 = -0.91$. Figure 8(b) shows the different contributions to the fit of the
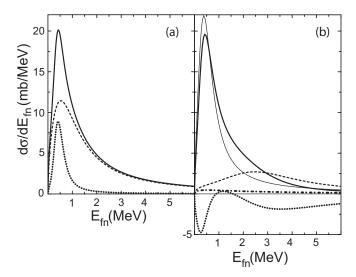

FIG. 8. Two different interpretations of a spectrum. (a) Part of $d\sigma/dE_{fn}$ described by the components 1 and 2 used in Fig. 3. A narrow p-wave resonance is superimposed on a broad s-wave resonance. The component with $\ell = 0$ is shown as a dashed line and the dotted line displays the $\ell = 1$ component. The solid line is a sum of the two components. (b) The result of a fit to the same spectrum as shown in (a) in the energy region $0 \leqslant E_{fn} < 3$ MeV assuming two $\ell = 0$ resonances in ^{13}Be. The spectrum corresponding to the decay of the first $1/2^+$ state by neutron emission to the ^{12}Be(g.s.) is shown as a thin solid line. The dashed line shows the spectrum from the decay of the second $1/2^+$ state to the ground state of ^{12}Be. The dashed-dotted line corresponds to the decay of the second $1/2^+$ state to the excited 0_2^+ state in ^{12}Be. The interference term is shown as a dotted line.

spectrum. The two resonances interfere destructively, shown as a dotted line, which is expected from the resonance structures of the two s states with configurations according to Eqs. (5) and (6). The positions of the corresponding S-matrix poles were found by solving $(E_{fn} - E_r)^2 + \frac{1}{4}\Gamma^2(E_{fn}) = 0$ for the two s states. One finds that both lie in the fourth quadrant of the complex energy plane, which shows that both are resonance states. A virtual state should have a pole at negative real energy. Note, a small contribution to the spectrum from the decay of the second $1/2^+$ state to the 0_2^+ state in ^{12}Be [shown as a dash-dotted line in Fig. 8(a)]. This is in agreement with the results in Refs. [20,70].

The shape of the spectrum from Fig. 8(a) was then used as an input to the fitting of the $d\sigma/dE_{fn}$ spectrum, instead of components 1 and 2, and with its amplitude as a free parameter. Furthermore, the amplitude of the $\ell = 2$ state at 5.2 MeV was taken as a free parameter. All other parameters were kept fixed

TABLE V. Parameters of the two $1/2^+$ resonances in ^{13}Be obtained from the fit. Resonance energies (E_r), resonance widths (Γ), and S-matrix poles (E_s) are given in MeV.

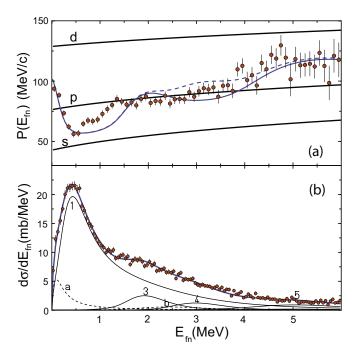|	$1/2_1^+$			$1/2_2^+$	
E_r	Γ	E_s	E_r	Γ	E_s
0.46	0.75	$0.30 - i0.34$	2.9	3.9	$2.2 - i1.8$

FIG. 9. (Color online) (a) Momentum profile of the ^{12}Be + n system after one-neutron knockout from ^{14}Be impinging on a hydrogen target at 304 MeV/nucleon. The solid line shows the calculated profile function obtained assuming two $\ell = 0$ resonances in ^{13}Be. The dashed line corresponds to the assumption that component 4 has $\ell = 2$ instead of $\ell = 1$. (b) ^{12}Be + n relative-energy spectrum from ^{1}H(^{13}Be,^{12}Be + n) at 304 MeV/nucleon obtained in the present experiment. The fit gave $\chi^2/N = 1.1$. The lines show the decomposition of the spectrum into individual resonances. Component 1 in this case describes the contribution from the two $\ell = 0$ resonances with destructive interference. The remaining notation is the same as in Fig. 3.

with values given in Table III. The fit resulted in $\chi^2/N = 1.1$ and is shown in Fig. 9(b) . From this one obtains an s-wave contribution of 28 mb, which includes 1.6 mb for the feeding to the 0^+ state in ^{12}Be. The cross section for the state at 5.2 MeV was increased by a factor 5 from 0.4 mb to 2 mb. This is removing the previously mentioned disagreement between the analysis of the transverse momentum distribution in $4 \leqslant E_{fn} \leqslant 6$ MeV shown in Fig. 5 and the result of the $d\sigma/dE_{fn}$ decomposition in Fig. 3(b).

The momentum-profile function obtained under the assumption of two $\ell = 0$ resonances in ^{13}Be shown as a solid line in Fig. 9(a) agrees much better with the experimental data as compared to the result given in Fig. 7. Both these observations favor the alternative interpretation of the low energy part of the $d\sigma/dE_{fn}$ spectrum.

There are still two regions of the profile function where there are relatively strong deviations between $P(E_{fn})$ and $P_{calc}(E_{fn})$. The deviation at 1 MeV may indicate the presence of an $\ell \neq 0$ resonance. The deviation around 3 MeV may be due to a $3/2^+$ resonance predicted in Ref. [70]. The dashed curve shown the resulting profile function under the assumption of an $\ell = 2$ for component 4 instead of $\ell = 1$. We can thus not exclude that there are overlapping $\ell = 1$ and 2 states in this region.

VI. DISCUSSION

The analysis presented in this paper gives the possibility to draw several conclusions about both the excited states in the unbound nucleus ^{13}Be and the ground-state wave function of ^{14}Be.

Our focus was to understand the new data from our one-neutron knockout experiment in the context of other existing results. We have analyzed the relative-energy spectrum from which the excited states in ^{13}Be may be deduced. The interpretation of the ℓ quantum numbers for the states have been supported by an analysis of the momentum distributions and in particular by studying the momentum profile function, which has a higher sensitivity to angular momentum content.

The relative-energy spectrum is very similar to those obtained in our previous experiment and in the similar experiment performed at lower energy at RIKEN. The shape of the spectrum is rather featureless with one broad maximum around 0.5 MeV and another less pronounced at about 3 MeV. In a recent paper [50] we showed that the energy region around 0.5 MeV in the relative-energy spectrum contained a very large s-wave component in contrast to what was found in the analysis by Kondo *et al.* [9].

A comparison of the relative-energy spectrum of ^{12}Be + n from proton knockout from ^{14}B and neutron knockout from ^{14}Be revealed a more narrow distribution at low energy for the latter. With a dominant structure of ^{14}B as ^{13}B($3/2^-$) $\otimes$ (sd) the low-energy peak may be assumed to be a relatively pure s state. A fit of the spectrum from Ref. [42] together with two resonances at 2 MeV ($5/2^+$) and 2.9 MeV ($1/2^-$) identified in earlier missing mass experiments given in Table I gave the resonance parameters for the low-energy s-wave resonance. The conclusion here is that a low-lying p state is essentially not populated in the proton knockout experiment.

Two other important pieces in the analysis were given by the neutron-gamma coincidence data from RIKEN, that revealed feeding to both the 2^+ state in ^{12}Be at 2.1 MeV and to the 1^- state at 2.7 MeV. The profile function analysis shows a strong increase at low relative energy and, as pointed out in Ref. [50], this may be due to knockout of an $\ell = 2$ neutron populating the $5/2^+$ state in ^{13}Be. This state, which lies close in excitation to the 2^+ state in ^{12}Be, is very likely to contain the configurations $[^{12}$Be(0^+) $\otimes d_{5/2}^+]$ and a core-excited component $[^{12}$Be(2^+) $\otimes s_{1/2}^+]$ (see Ref. [61]). The tail of the latter may decay by s-wave neutrons to the 2^+ state. The observation of Ref. [9] that the neutrons in coincidence with the 2.1 MeV gammas were of very low energy supports this conclusion. The deduced branching ratio of the decay to the ground state and the excited state in ^{12}Be is ~50%.

The E_{fn} spectrum obtained in the triple coincidence experiment in Refs. [9,10], ^{12}Be + n + 2.7 MeV γ rays, proves the existence of a state in ^{13}Be at $E_r = 5.2(1)$ MeV [$\Gamma = 1.4(2)$ MeV] decaying to the ^{12}Be(1^-) state. This might originate from the decay of a $3/2^-$ state by emission of an $\ell = 0$ neutron.

In the missing mass experiment [31] a low energy state was observed at an energy of 0.80(9) MeV. The resolution in the experiment, as reported in Ref. [31], is about 0.7 MeV and thus does not allow to clearly distinguish whether the spectral shape

corresponds to $I^\pi = 1/2^+$ or $1/2^-$. It is, however, unlikely that the peak at 0.80(9) MeV would be the same as in the present experiment at 0.46(1) MeV. The positions differ by more than 2σ. This state was therefore not considered in the analysis presented here.

The analysis assuming two low-energy states with $\ell = 0$ and $\ell = 1$, an $\ell = 2$ resonance around 2 MeV, an $\ell = 1$ resonance at about 3 MeV, and a structure around 5 MeV together with the contributions from the decays to the excited 2^+ and 1^- states in ^{12}Be gave an excellent fit to the relative-energy spectra at the two energies 69 MeV/nucleon and 304 MeV/nucleon. Furthermore, the obtained cross section ratio between the two experiments were found to stay constant for all states included in the fit and to be in good agreement with the value expected from a comparison with total (p, n) cross sections.

Already at this point in the investigation, the data give evidence for an s-wave dominance at low energy amounting to about 60%. The possible p state gave a contribution around 16%.

The profile function calculated using the parameters from the fit provided, however, not a satisfactory agreement with the experimental shape at low energy, where a stronger decrease was observed, and in the region between 4 and 6 MeV, where the experimental profile function signaled a stronger d contribution.

A new analysis, with the assumption of an excited $1/2^+$ state in the region around 3 MeV and interference between this state and the low energy $1/2^+$ state resulted in a satisfactory fit to the spectrum. The decay of the second $1/2^+$ state leads dominantly to the ^{12}Be ground state. This is in agreement with estimates based on Refs. [20,70] mentioned above. This gave a total contribution to the spectrum from the two s states of about 75% s and a contribution from the high-energy d state of about 5%. No contribution from a low-lying p state was needed to reproduce the relative energy spectrum.

VII. SUMMARY

We have presented an analysis of a one-neutron knockout experiment from 304 MeV/nucleon ^{14}Be impinging on a liquid hydrogen target. The analysis was performed including all existing, published experimental data. A consistent description

for the excited states in ^{13}Be was obtained. The following observations have been made:

   (i) The impulse approximation formalism described by a Feynman diagram with two vertices is found to be an appropriate description of neutron knockout reactions at both 69 and 304 MeV/nucleon beam energies.

   (ii) The dominating component in the ^{12}Be + n relative-energy spectrum is an s wave with at least ∼60% of the total intensity.

  (iii) A remarkable result is the indication that the narrow component at 0.44 MeV in the decomposition of $d\sigma/dE_{fn}$, proposed in Refs. [9,37] and in the present experiment, might be explained with the inclusion of a second excited s-wave component.

   (iv) An observed resonance at 0.80(9) MeV [31] in the missing-mass experiments and another at 0.65(10) [30] cannot be seen in the ^{13}Be + n relative energy spectra. However, the comparison between experimental and calculated momentum profiles shown in Fig. 9(a) still leaves a possibility that an $\ell \neq 0$ resonance at around 1 MeV might exist.

   (v) The decay of the $5/2^+$ state at 2 MeV populates both the ground state and the 2^+ state at 2.1 MeV in ^{12}Be with a branching ratio of about 50%.

   (vi) The difference in the interpretations of the ^{13}Be structure obtained in experiments using the invariant-mass and the missing-mass methods is resolved in the present analysis by including all existing experimental data.

[1] *Proceedings of the Nobel Symposium NS 152* [C. Fahlander and B. Jonson (eds.), Phys. Scr. T **152**, 1 (2013)].

[2] H. Simon, Phys. Scr. T **152**, 014024 (2013).

[3] A. Bonaccorso, Phys. Scr. T **152**, 014019 (2013).

[4] Yu. Aksyutina *et al.*, Phys. Lett. B **666**, 430 (2008).

[5] A. Spyrou, Z. Kohley, T. Baumann, D. Bazin, B. A. Brown, G. Christian, P. A. DeYoung, J. E. Finck, N. Frank, E. Lunderberg, S. Mosby, W. A. Peters, A. Schiller, J. K. Smith, J. Snyder, M. J. Strongman, M. Thoennessen, and A. Volya, Phys. Rev. Lett. **108**, 102501 (2012).

[6] C. Forssén, G. Hagen, M. Hjorth-Jensen, W. Nazarewicz, and J. Rotureau, Phys. Scr. T **152**, 014022 (2013).

[7] K. Riisager, Phys. Scr. T **152**, 014001 (2013).

[8] M. V. Zhukov, B. V. Danilin, D. V. Fedorov, J. M. Bang, I. J. Thompson, and J. S. Vaagen, Phys. Rep. **231**, 151 (1993).

[9] Y. Kondo *et al.*, Phys. Lett. B **690**, 245 (2010).

[10] Y. Kondo, Spectroscopy of ^{13}Be and ^{14}Be via proton-induced breakup reactions, Ph.D. thesis, Department of Physics, Tokyo Institute of Technology, 2007.

[11] H. O. U. Fynbo, Phys. Scr. T **152**, 014010 (2013).

[12] Y. Parfenova and Ch. Leclercq-Willain, Phys. Rev. C **72**, 024312 (2005).

[13] O. Burda, P. von Neumann-Cosel, A. Richter, C. Forssén, and B. A. Brown, Phys. Rev. C **82**, 015808 (2010).

[14] E. Garrido, D. V. Fedorov, and A. S. Jensen, Phys. Lett. B **684**, 132 (2010).

[15] J. N. Orce *et al.*, Phys. Rev. C **86**, 041303(R) (2012).

[16] T. Otsuka, N. Fukunishi, and H. Sagawa, Phys. Rev. Lett. **70**, 1385 (1993).

[17] H. Esbensen, B. A. Brown, and H. Sagawa, Phys. Rev. C **51**, 1274 (1995).

[18] J. S. Winfield *et al.*, Nucl. Phys. A **683**, 48 (2001).

[19] K. T. Schmitt *et al.*, Phys. Rev. Lett. **108**, 192701 (2012).

[20] F. C. Barker, J. Phys. G: Nucl. Part. Phys. **36**, 038001 (2009).

[21] A. Krieger, K. Blaum, M. L. Bissell, N. Frömmgen, Ch. Geppert, M. Hammen, K. Kreim, M. Kowalska, J. Kramer, T. Neff, R. Neugart, G. Neyens, W. Nörtershäuser, Ch. Novotny, R. Sánchez, and D. T. Yordanov, Phys. Rev. Lett. **108**, 142501 (2012).

[22] F. M. Nunes, I. J. Thompson, and J. A. Tostevin, Nucl. Phys. A **703**, 593 (2002).

[23] C. Romero-Redondo, E. Garrido, D. V. Fedorov, and A. S. Jensen, Phys. Lett. B **660**, 32 (2008); Phys. Rev. C **77**, 054313 (2008).

[24] C. Forssén, V. D. Efros, and M. V. Zhukov, Nucl. Phys. A **706**, 48 (2002).

[25] P. Descouvemont, Phys. Rev. C **52**, 704 (1995).

[26] I. J. Thompson and M. V. Zhukov, Phys. Rev. C **53**, 708 (1996).

[27] M. Labiche, F. M. Marques, O. Sorlin, and N. Vinh Mau, Phys. Rev. C **60**, 027303 (1999).

[28] T. Tarutina, I. J. Thompson, and J. A. Tostevin, Nucl. Phys. A **733**, 53 (2004).

[29] D. V. Aleksandrov, E. A. Ganza, Yu. A. Glukhov, V. I. Dukhanov, I. B. Mazurov, B. G. Novatsky, A. A. Ogloblin, D. A. Stepanov, V. V. Paramonov, and A. G. Trunov, Yad. Fiz. **37**, 797 (1983) [Sov. J. Nucl. Phys. **37**, 474 (1983)].

[30] M. G. Gornov, Yu. B. Gurov, S. V. Lapushkin, P. V. Morokhov, V. A. Pechkurov, K. Seth, T. Pedlar, J. Wise, and D. Zhao, Bull. Russ. Acad. Sci. Phys. **62**, 1781 (1998).

[31] A. V. Belozyorov, R. Kalpakchieva, Yu. E. Penionzhkevich, Z. Dlouh, S. Pisko, J. Vincour, H. G. Bohlen, M. von Lucke-Petsch, A. N. Ostrowski, D. V. Alexandrov, E. Yu. Nikolskii, B. G. Novatskii, and D. N. Stepanov, Nucl. Phys. A **636**, 1781 (1998).

[32] A. N. Ostrovski, H. G. Bohlen, A. S. Demyanova, B. Gebauer, R. Kalpakchieva, Ch. Langner, H. Lenske, M. von Lucke-Petsch, W. von Oertzen, A. A. Ogloblin, Y. E. Penionzhkevich, M. Wilpert, and Th. Wilpert, Z. Phys. A **343**, 489 (1992).

[33] A. A. Korsheninnikov, E. Yu. Nikolskii, T. Kobayashi, D. V. Aleksandrov, M. Fujimaki, H. Kumagai, A. A. Ogloblin, A. Ozawa, I. Tanihata, Y. Watanabe, and K. Yoshida, Phys. Lett. B **343**, 53 (1995).

[34] Y. Blumenfeld, T. Nilsson, and P. Van Duppen, Phys. Scr. T **152**, 014023 (2013).

[35] G. Randisi, Ph.D. thesis, Stucture des systèmes non liés ^{10,11}Li et ^{13}Be, Université de CAEN/BASSE-NORMANDIE, 2011, http://tel.archives-ouvertes.fr/tel-00656582/.

[36] J. L. Lecouey, Few-Body Syst. **34**, 21 (2004).

[37] H. Simon *et al.*, Nucl. Phys. A **791**, 267 (2007).

[38] S. Shimoura *et al.*, Phys. Lett. B **560**, 31 (2003).

[39] J. Johansen, dissertation, Aarhus Univesity, 2012, http://pure.au.dk/portal/files/50742308/Dissertation.pdf.

[40] V. Guimarães, J. J. Kolata, D. Bazin, B. Blank, B. A. Brown, T. Glasmacher, P. G. Hansen, R. W. Ibbotson, D. Karnes, V. Maddalena, A. Navin, B. Pritychenko, B. M. Sherrill, D. P. Balamuth, and J. E. Bush, Phys. Rev. C **61**, 064609 (2000).

[41] S. Takeuchi *et al.*, Phys. Lett. B **515**, 255 (2001).

[42] M. Labiche *et al.*, Phys. Rev. Lett. **86**, 600 (2001).

[43] A. Bohr and B. R. Mottelson, *Nuclear Structure* (W.A. Benjamin, Inc., Amsterdam, New York, 1969), Vol. I, p. 441.

[44] D. Overway, J. Jänecke, F. D. Bechetti, C. E. Thorn, and G. Kekelis, Nucl. Phys. A **366**, 299 (1981).

[45] Th. Blaich *et al.*, Nucl. Instrum. Methods Phys. Res. A **314**, 136 (1992).

[46] A. M. Lane and R. G. Thomas, Rev. Mod. Phys. **30**, 257 (1958).

[47] G. Audi, A. H. Wapstra, and C. Thibault, Nucl. Phys. A **729**, 337 (2003).

[48] H. T. Johansson *et al.*, Nucl. Phys. A **842**, 15 (2010).

[49] G. Blanchon, A. Bonaccorso, D. M. Brink, A. Garsía-Camacho, and N. Vinh Mau, Nucl. Phys. A **784**, 49 (2007).

[50] Yu. Aksyutina *et al.*, Phys. Lett. B **718**, 1309 (2013).

[51] W. P. Abfalterer, F. B. Bateman, F. S. Dietrich, R. W. Finlay, R. C. Haight, and G. L. Morgan, Phys. Rev. C **63**, 044608 (2001).

[52] Z. X. Cao *et al.*, Phys. Lett. B **707**, 46 (2012).

[53] Yu. Aksyutina *et al.*, Phys. Lett. B **679**, 191 (2009).

[54] A. W. Stetz, Phys. Rev. C **21**, 1979 (1980).

[55] P. G. Hansen, Phys. Rev. Lett. **77**, 1016 (1996).

[56] D. Bazin, W. Benenson, B. A. Brown, J. Brown, B. Davids, M. Fauerbach, P. G. Hansen, P. Mantica, D. J. Morrissey, C. F. Powell, B. M. Sherrill, and M. Steiner, Phys. Rev. C **57**, 2156 (1998).

[57] T. Aumann, L. V. Chulkov, V. N. Pribora, and M. H. Smedberg, Nucl. Phys. A **640**, 24 (1998).

[58] M. Zahar, M. Belbot, J. J. Kolata, K. Lamkin, R. Thompson, N. A. Orr, J. H. Kelley, R. A. Kryger, D. J. Morrissey, B. M. Sherrill, J. A. Winger, J. S. Winfield, and A. H. Wuosmaa, Phys. Rev. C **48**, R1484 (1993).

[59] A. Ozawa, T. Suzuki, and I. Tanihata, Nucl. Phys. A **693**, 32 (2001).

[60] S. Ilieva *et al.*, Nucl. Phys. A **875**, 8 (2012).

[61] H. T. Fortune and R. Sherr, Phys. Rev. C **82**, 064302 (2010).

[62] A. Navin *et al.*, Phys. Rev. Lett. **85**, 266 (2000).

[63] S. D. Pain *et al.*, Eur. Phys. J. A **25**, 349 (2005).

[64] S. Shimoura *et al.*, Phys. Lett. B **654**, 87 (2007).

[65] R. Kanungo *et al.*, Phys. Lett. B **682**, 391 (2010).

[66] T. Suzuki and T. Otsuka, Phys. Rev. C **56**, 847 (1997).

[67] H. T. Fortune and R. Sherr, Phys. Rev. C **74**, 024301 (2006).

[68] H. T. Fortune and R. Sherr, J. Phys. G **36**, 038002 (2009).

[69] G. Blanchon, N. V. Mau, A. Bonaccorso, M. Dupuis, and N. Pillet, Phys. Rev. C **82**, 034313 (2010).

[70] H. T. Fortune, Phys. Rev. C **87**, 014305 (2013).